ISSN impresa 0717-3644
ISSN online 0718-221X

Maderas. Ciencia y tecnología 18(4): 607 - 616, 2016
DOI: 10.4067/S0718-221X2016005000053

CO_2 ADSORPTION ON AGRICULTURAL BIOMASS COMBUSTION ASHES

Sebastián Lira-Zúñiga[1,♠], César Sáez-Navarrete[1], Leonardo Rodríguez-Córdova[1], Leandro Herrera-Zeppelin[2], Ronaldo Herrera-Urbina[3]

ABSTRACT

Carbon capture and storage has become an alternative means of confronting global warming. Further research and development into adequate and low-cost materials is required for CO_2 adsorption technologies.

Samples of fly ash, bottom ash and their respective pellets, produced from wheat bran combustion, were characterized and tested to assess their capacity for CO_2 adsorption at different temperatures. Neither the ashes nor their pellets were subject to prior thermochemical activation.

The bottom ash sample and its pellets showed a higher adsorption capacity for the majority of the temperatures studied. The pelletized bottom ash reached the maximum adsorption capacity (0,07 mmol CO_2/g), followed by the non-pelletized bottom ash (0,06 mmol CO_2/g); both at an adsorption temperature of 25°C.

CO_2 adsorption of bottom ash, from the combustion of wheat bran (agricultural biomass), by a physical adsorption mechanism was demonstrated whereas with the fly ash sample, CO_2 adsorption by both physical and chemical adsorption mechanisms was identified.

Keywords: Bottom ash, CO_2 capture, fly ash, pellet, wheat bran.

INTRODUCTION

The reduction of CO_2 emissions in order to stabilize global warming has become a contemporary challenge (Hoyos Barreto *et al*. 2008, Da Gama *et al.* 2010, Wilcox 2012). Nowadays, research into Carbon Capture and Storage (CCS) technologies is a topic of worldwide interest, as it can be used to capture CO_2 emissions from fossil fuel power plants.

[1]Departamento de Ingeniería Química y Bioprocesos, Pontificia Universidad Católica de Chile, Santiago. Chile.
[2]Departamento de Ingeniería Química y Biotecnología, Universidad de Chile, Santiago. Chile.
[3]Departamento de Ingeniería Química y Metalúrgica, Universidad de Sonora, México.
♠ Corresponding author: snlira@uc.cl
Received: 03.12.2015 Accepted: 16.07.2016

The main carbon capture technologies are based on systems of absorption, adsorption and on membrane separation and cryogenic distillation technologies. The process based on adsorption phenomena is considered to be one of the most promising technologies in terms of capturing CO_2 from combustion gases (Arenillas *et al.* 2005), giving rise to the possibility of an efficient separation in diluted gas mixtures (Wilcox 2012). Within this context, it is important to note the study of new low-cost adsorbents (Boumediene *et al.* 2015) which may hold significant CO_2 adsorption capacities.

Combustion coal and agricultural biomass ashes provide a viable alternative, are low-cost and have the potential to capture the CO_2 produced by combustion gases because of these byproducts contain significant amount of reactive metal oxides (Wilcox 2012).

The ashes produced from coal combustion are chemically heterogeneous amorphous solids. Their physicochemical properties depend on the conditions of the combustion process itself and the type of fuel being used (Amaya 2006). Ashes are common industrial-sourced alkaline byproduct (Gerdemann *et al.* 2007, Wilcox 2012). They contain about 90% and 99% inorganic compounds and between 1% and 9% organic compounds (Vassilev 2005). The main inorganic substances of coal combustion ashes are silicon dioxide (SiO_2), calcium oxide (CaO), iron oxide (Fe_2O_3), magnesium oxide (MgO) and aluminium oxide (Al_2O_3) (Hong *et al.* 2009, Malik and Thapliyal 2009, Wilcox 2012). Agricultural biomass combustion ashes have not been thoroughly characterized, even though they may represent a viable alternative for CCS applications.

In 2012 the United States produced approximately 52,1 million tonnes of fly ash, 14,1 million tonnes of bottom ash and 1,7 million tonnes of slag (ACAA 2012) in coal-based energy generation alone. In 2007, Eastern Europe produced 4,6 million tonnes of coal fly ash 5,7 million tonnes of coal bottom ash and 1,5 million tonnes of boiler slag (ECOBA 2007). As a consequence of the increased amount of ash generated over the last few decades (ACAA 2012), the search for new alternatives of energy recovery has widened.

Moreover, new alternatives biomass fuels are widely used in combustion processes and biomass ashes generated are becoming a burgeoning problem (Torres-Fuchslocher y Varas-Concha 2015). This search is aimed at reducing the environmental impacts that stem from the inappropriate management of these waste materials(Arenillas *et al*. 2005, Maroto-Valer *et al*. 2005, Hong *et al.* 2009, Ríos *et al.* 2009, Lopez-Anton *et al*. 2011).

In this research work, two types of ash samples from the combustion of agricultural biomass (wheat bran), in powder and pellet forms, were characterized and tested as CO_2 adsorbents. The ash samples tested were the following: fly ash (FA), pelletized fly ash (PFA), bottom ash (BA) and pelletized bottom ash (PBA). Their CO_2 adsorption capacity and degree of reversibility were evaluated, and their physicochemical characterization enabled identification of the main CO_2 adsorption mechanisms.

MATERIALS AND METHODS

Fly ash (FA), bottom ash (BA) and their respective pellets were studied (PFA and PBA). FA and BA samples of wheat bran combustion were obtained through an industrial biomass boiler (4000 kcal/h). Pellets measuring 5mm in diameter were prepared at 200 psi for all samples (Napoli NP-RD10A). The samples tested were not subject to chemical or thermal activation.

The relative constituent oxides of the two ash samples were used to calculate their corresponding chemical composition.

The specific surface area of the two types of ash and their respective pellets was determined from nitrogen adsorption isotherms at -196°C, using an ASAP 2010 Micrometrics sorptometer.

The BET method (Brunauer *et al.* 1938) was used to calculate the specific surface area (S_{BET}). Using data from the BET isotherm, both the pore and micropore volumes were established. The pore volume ranging from 1,7 nm to 300 nm was determined by using the BJH method (Barrett *et al.* 1951). The micropore volume, on the other hand, was calculated using the t-plot method. By taking both the specific surface area and the pore volume into account, the average pore size was calculated using the equation $4V_{total}/S_{BET}$.

CO_2 adsorption mechanisms on FA and BA were identified using data from the N_2 adsorption isotherm at -196°C. Additionally, the research demonstrated whether or not these mechanisms were modified by the pelletization process of both samples (PFA and PBA).

The general morphology and porous structure of the ash samples and their pellets were characterized by means of scanning electron microscopy SEM (LEO VP 1400).

The adsorption capacity of the ashes and their pellets at different temperatures (25°C, 40°C, 60°C, 80°C and 100°C) was investigated using a TG Q500 thermogravimetric analyzer (TGA), with a sample capacity of 20-25 mg.

To determine the initial conditions for the adsorption capacity of the ashes, a flow of N_2 (100% w/w) was introduced at a rate of 100 mL/min and at a temperature of 100°C for 30 minutes. This was subsequently adjusted to the required adsorption temperature, prior to the introduction of a CO_2 flow (at 100% w/w concentration) at a rate of 100 mL/min. After adsorption, a new flow of N_2 at a rate of 100 mL/min was again introduced to initiate desorption of the sample at the same temperature. The adsorption capacity was calculated from the results of gravimetric analyses.

RESULTS AND DISCUSSION

Table 1 shows the main alkaline oxides (K_2O; CaO; MgO; SiO_2, Na_2O; Al_2O_3; Fe_2O_3 and MnO) of the ash samples studied. Also shows significant differences can be seen between the amount of the principal metal oxides present in FA and BA samples. In addition, this table shows the notable presence of volatile components (LOI, Loss on Ignition).

Table 1. Main components of FA and BA ash samples.

wt%	LOI	K_2O	CaO	MgO	SiO_2	Na_2O	Al_2O_3	Fe_2O_3	MnO
FA	7,28	38,72	1,18	2,54	28,2	0,32	0,09	0,12	0,10
BA	1,48	25,32	2,02	16,42	15,19	0,16	0,88	0,38	0,32

The texture characterization results (Table 2), show that the BA sample presents greater specific surface area than the FA. It can be noted that the pelletization process reduces the specific surface area of both samples, to 34% for the FA and to 58,3% for the BA.

Table 2. Texture properties of ash and pellet samples determined from N_2 adsorption isotherms.

Sample	S_{BET} (m^2/g)	$Area_{micro}$ (m^2/g)	V_{micro} (cm^3/g)	Pore Size (nm)	PoreVolume (cm^3/g)
FA	5,0	0,76	0,000242	5,61	0,007
PFA	1,7	0,05	0,000030	4,31	0,002
BA	12,0	4,24	0,002	3,1	0,009
PBA	7,0	2,43	0,001	3,8	0,006

By comparing the specific surface area of these ash samples with commercial adsorbents, activated carbon with large pores was found to have a specific surface area in the range of 200-600 m^2/g (Wilcox 2012), a value significantly higher than the samples studied here. However, there are commercial adsorbents with similar specific surface areas to the mesoporous activated carbon, with values ranging from 10-100 m^2/g (Sanz 2012), as well as resins, which have specific surface areas between 15 and 120 m^2/g (Wilcox 2012). Such values coincide with the lower range of the specific surface area of both the aforementioned commercial adsorbents.

The microporosity per unit of the pore volume ratio means that the BA consists of 22% micropores, the PBA 17%, the FA 3,5% and the PFA 1,5%. Therefore, the specific surface area of the BA was composed of 2,64 m^2/g micropores and 9,36 m^2/g mesopores. The PBA contained 1,19 m^2/g of micropores and 5,81 m^2/g of mesopores. The specific surface area of the FA was composed of 0,18 m^2/g micropores and 4,83 m^2/g mesopores, while the PFA was 0,03 m^2/g micropores and 1,70 m^2/g mesopores. These results provide evidence of a greater presence of micropores in the BA and PBA samples.

Table 2 also shows that the pore size was not affected by the samples undergoing pelletization. For the large-pore activated carbon, the resins, the activated alumina (Wilcox 2012), the mesocarbon and the graphene (Chen - Hsiu. 2012), a pore size similar to the ash samples and their respective pellets was documented.

According to the pore size result, all the FA, BA, PFA and PBA are mesoporous solids, given that their registered pore sizes ranged from between 2 nm and 50 nm. All the samples studied fell into the lower range of pore size according to IUPAC (International Union of Pure and Applied Chemistry) classification (Table 2). It is important to note that the kinetic diameter of CO_2 (0,33 nm) is smaller than the diameter of FA, PFA, BA and PBA pores.

The kinetic diameter of CO_2 is similar to most of the gas species present in the gas mixture of interest (typical gas- mixture components include N_2, O_2 and CH_4), and consequently CO_2 tends to be more reactive than these species due to its stronger quadrupole moment, making it an easier target for selective capture (Wilcox 2012).

Given the pore size, the predominant mechanism of internal transport for the FA, BA, PFA and PBA was the Knudsen diffusion. This is instead of free molecular diffusion and surface diffusion, in which the free motion of the molecules in the gaseous phase is greater than the pore diameter. Here, conditions can lead to molecules colliding with the internal pore walls rather than collisions occurring between the gas molecules. This type of internal diffusion mechanism is typical of mesoporous and microporous solids (Castañeda 2012).

The porous structure highlighted by SEM analysis shows that the FA (Figure 1) and the BA (Figure 3) can be considered amorphous and heterogeneous solids. The SEM analysis shows changes to the structure of the PFA pellet (Figure 2) compared to the FA, and likewise the PBA pellet (Figure 4) compared to the BA. Nevertheless, they retain their amorphous and heterogeneous solid condition.

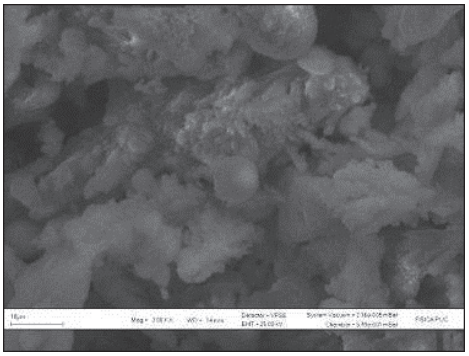

Figure 1. SEM image of FA sample (3KX).

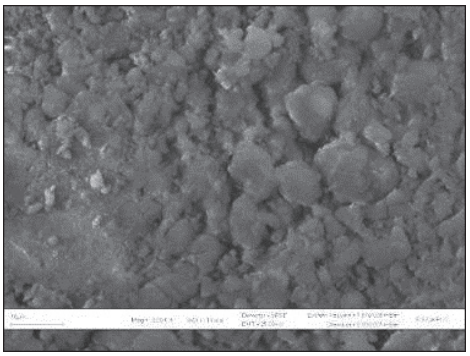

Figure 2. SEM image of PFA sample (3KX).

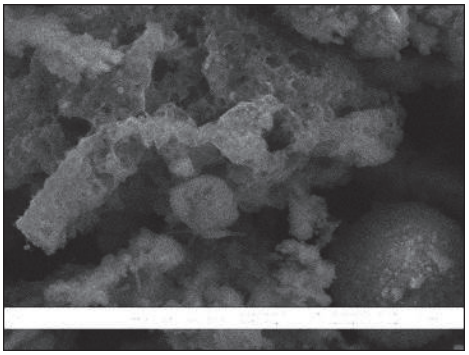

Figure 3. SEM image of BA sample (3KX).

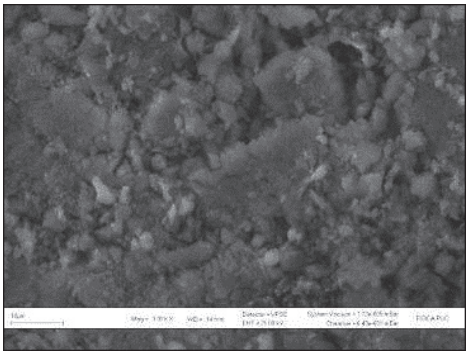

Figure 4. SEM image of PBA sample (3KX).

According to IUPAC classification, the N_2 adsorption isotherm at -196°C for the BA and PBA samples, corresponds to isotherm type IV (Figure 5). This type of isotherm is common in mesoporous solids, in which multilayer physical adsorption mechanisms predominate. The type 4 isotherm is similar in form to that of type II at low pressures. A distinctive feature of this type of isotherm is its hysteresis loop. The isotherm for the FA and PFA samples corresponds to a type II isotherm (Figure 6). This type of isotherm is present in macroporous solids in which multilayer adsorption mechanisms predominate.

Figure 5 indicates that the volume of adsorbed N_2 on the BA sample is greater than that of the PBA sample. In addition, the BA and PBA isotherms show a hysteresis loop under medium relative pressures (p/p_0 =0,45). This confirms the presence of mesopores in both ash types.

Both the BA and PBA samples showed a rapid increase of nitrogen adsorption under very low relative pressures ($p/p_0 < 0,01$). This process is typical of molecular-sized pores and indicates the existence of micropores. This latter point confirms, once more, the presence of micropores in both samples.

In the region of relative pressures, between p/p_0 = 0,01-0,45 the amount of adsorbed nitrogen on the BA and PBA samples (Figure 5) and the FA sample (Figure 6), increases slowly and progressively. This type of surface adsorption process indicates a monolayer formation.

In the region of elevated relative pressures ($p/p_0 > 0,45$) the BA and PBA isotherms are characterized by the presence of hysteresis loop. The hysteresis loop arises because of the process whereby the mesopores in these samples are filled. This is controlled by the phenomenon of capillary condensation (an irregular size of capillaries) as well as by the percolation properties of the solid.

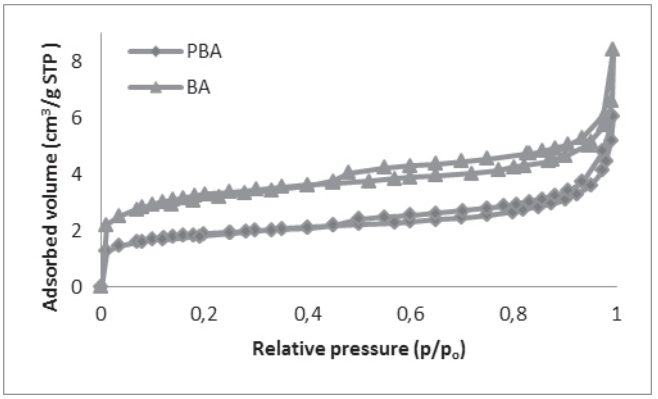

Figure 5. N_2 adsorption isotherm at -196 °C for BA and PBA.

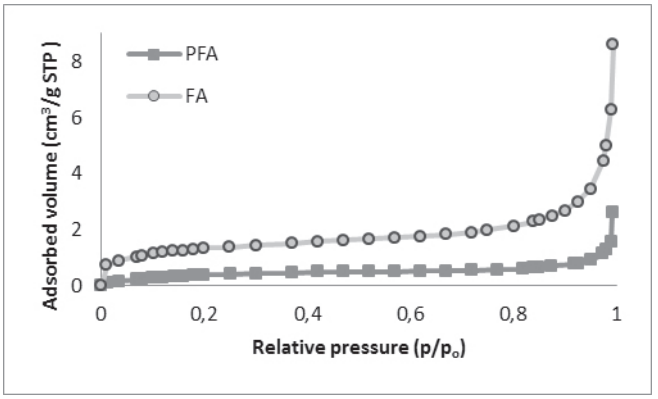

Figure 6. N_2 adsorption isotherm at -196 °C for FA and PFA.

The adsorption capacity of the four different samples of wheat bran ash tested in this research is presented in Figures 7 and 8 at five different temperatures. In powder form, the BA sample exhibits the greatest CO_2 adsorption capacity at an adsorption temperature of 25°C, reaching 0,06 mmol of CO_2/g (Figure 7), whereas the FA sample displays the greatest CO_2 adsorption capacity at the adsorption temperature of 100°C, capturing 0,024 mmol of CO_2/g (Figure 8). Furthermore, the BA sample exhibits a greater CO_2 adsorption capacity in the majority of the adsorption temperatures investigated. Only at a temperature of 100°C did the FA display a greater capacity than the BA.

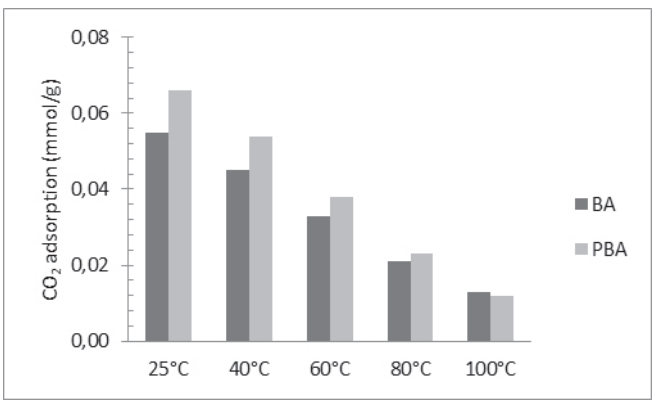

Figure 7. CO_2 adsorption capacity of BA and PBA at different temperatures.

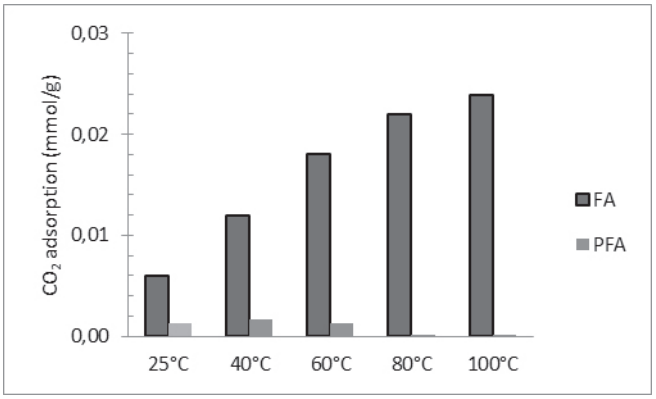

Figure 8. CO_2 adsorption capacity of FA and PFA at different temperatures.

Figure 7 also shows that the CO_2 adsorption capacity of the BA decreased when the adsorption temperature was increased. Therefore, this confirms that the dominant adsorption mechanism in the BA sample was one of physical adsorption (Maroto-Valer *et al.* 2005). In relation to FA, Figure 8 shows that an increment in temperature increases CO_2 adsorption capacity, suggesting that not only physical adsorption but also chemical adsorption could be occurring (Maroto-Valer *et al.* 2005). Alkaline metal oxide (such as K_2O) might react with CO_2 and produce K_2CO_3 at higher temperatures (Yong *et al.* 2002). It is probable that the existence of some kind of alkaline functional group on the surface, such as the K_2O corresponding to the FA, could explain the increased CO_2 adsorption capacity when the adsorption temperature is raised. This could be confirmed by research with amine impregnated adsorbent (polyethylenimine or PEI). This would indicate whether, by raising the adsorption temperature from 25°C to 75°C, it would be possible to increase CO_2 adsorption capacity (Chen - Hsiu. 2012). When an adsorbent presents alkaline compounds on the surface, a part of this material is accumulated inside the pore at low temperatures, limiting the CO_2 diffusion process. At high temperatures, the alkaline functional groups may not accumulate in the pores, allowing for a high diffusion rate of CO_2. This increases the reaction rate of CO_2 with the alkaline compounds distributed into the interior of the pores, resulting in an increase of the CO_2 adsorption capacity (Sayari 2010).

Regarding the pellets, the adsorption capacity decreased in the PFA compared to that of the FA. In addition, it behaved differently to the FA following the increase of the adsorption temperature. The pelletization of the FA seems to have changed the structure of the pores, which affected access to the active adsorption sites and, therefore, its CO_2 adsorption capacity.

Just as with the BA, the PBA registered a decrease in its CO_2 adsorption capacity following the increase of the adsorption temperature. However, in contrast to the FA, the CO_2 adsorption capacity of the PBA rose slightly compared to that of the BA. The decrease in adsorption capacity following a temperature increase corresponds to a classic physical adsorption mechanism. Here, an increase in temperature disturbs the surface stability of the CO_2 molecule, causing its liberation by increasing surface adsorption energy and the molecular diffusion rate (Maroto-Valer *et al.* 2005). Adsorbents like zeolites, activated carbons (Xu *et al.* 2002) and anthracites (Maroto-Valer *et al.* 2005) have also demonstrated such behaviour.

The maximum CO_2 adsorption capacities registered by the BA and PBA are comparable (0,06 and 0,07 mmol of CO_2/g respectively) with that of other solids at the adsorption temperature of 25°C. Both samples exhibit an adsorption capacity of 0,09 mmol of CO_2/g (Arenillas *et al.* 2005), similar to that of raw coal. Furthermore, this is greater than the adsorption capacity of commercial adsorbents like mesoporous silica (MCM-41), which can reach a capacity of 0,04 mmol of CO_2/g (Yue *et al.* 2006). Activated carbon has an adsorption capacity of 1,66 mmol CO_2/g (Pevida *et al.* 2008), which is substantially higher than that of the samples studied in this research work. Given that they require no activation, unlike other commercial absorbents, the BA and PBA could have future potential as low-

cost adsorbents.

The adsorption capacity of fly ash with a high content of partially combusted coal has generated values between 0,39 and 0,915 mmol CO_2/g (Maroto-Valer *et al.* 2008) at an adsorption temperature of 30°C. These are higher than the BA and PBA values, given the high content of uncombusted carbon in the latter.

As mentioned previously, BA (12 m^2/g) and PBA (7 m^2/g) have small specific surface areas compared to certain commercial adsorbents. Solids such as anthracite, with a small specific surface area and high CO_2 adsorption capacity, present a specific surface area of 1,34 m^2/g and an adsorption capacity of 0,868 mmol of CO_2/g (Maroto-Valer *et al.* 2008).

CONCLUSIONS

Fly ash and bottom ash samples produced by an industrial process of wheat bran agricultural biomass combustion, in unprocessed powder and pelletized forms, have been physically and chemically characterized.

The study of N_2 adsorption at -196°C has shown that the BA and PBA samples are mainly composed of mesoporous solids (with pores sizes of 2 - 50 nm), while the FA and PFA samples are primarily macroporous solids (with pores greater than 50 nm).

The BA presented the largest specific surface area (12 m^2/g), followed by the PBA pelletized form (7 m^2/g).

CO_2 adsorption on BA involves a physical adsorption mechanism, given that its CO_2 adsorption capacity decreased following an increase of the adsorption temperature. This mechanism was also displayed by the PBA sample. On the other hand, the FA samples showed the presence of both physical and chemical adsorption mechanisms. As a result of the pelletization process, the CO_2 adsorption capacity of the PFA sample was reduced significantly.

The greatest CO_2 adsorption capacity was obtained with the PBA sample, reaching 0,07 mmol of CO_2/g at 25 °C. A similar CO_2 adsorption capacity was obtained by the BA at 25°C (0,06 mmol of CO_2/g).

The PBA pelletized form of the bottom ash from the wheat bran agricultural biomass combustion therefore showed characteristics which could result in its use as an efficient and low-cost adsorbent for the capture of CO_2.

ACKNOWLEDGMENTS

The authors wish to express their thanks to Dr. Paulo Araya (Department of Chemical Engineering, Universidad de Chile) and Dr. Trevor Drage (Department of Chemical and Environment Engineering, University of Nottingham) for their valuable contributions to this study.

This research was supported partially by the National Commission for Scientific and Technological Research (Comisión Nacional de Investigación Científica y Tecnológica, CONICYT) of the Chilean Government via a doctoral scholarship awarded to Sebastián Lira-Zúñiga (No.21100358) and Leonardo Rodríguez-Córdova (No. 21090472).

REFERENCES

ACAA. 2012**.** Coal Combustion Products Survey. [online]<https://www.acaa-usa.org/Portals/9/Files/PDFs/revisedFINAL2012CCPSurveyReport.pdf>[november 11th 2013].

Amaya, J.T.A.; Sánchez, F. 2006. Employing fly ash and FCC catalyser waste in recovering chrome (III) from liquid effluent emitted by tanneries. *Ingeniería e Investigación* 25(57):39-48.

Arenillas, A.; Smith, K.M.; Drage, T.C.; Snape, C.E. 2005. CO_2 capture using some fly ash-derived carbon materials. *Fuel* 84(17): 2204-2210.

Barrett, E.; Joyner, L.; Halenda, P. 1951. The determination of pore volume and area distributions in porous substances. I. Computations from nitrogen isotherms. *Journal of the American Chemical Society* 73(1):373-380.

Boumediene, M.; Benaïssa, H.; George, B.; Molina, S.; Merlin, A. 2015. Characterization of two cellulosic waste materials (orange and almond peels) and their use for the removal of methylene blue from aqueous solutions. *Maderas. Ciencia y tecnología* 17(1):69-84.

Brunauer, S.; Emmett, P.; Teller, E. 1938. Adsorption of gases in multimolecular layers. *Journal of the American Chemical Society* 60(2)**:**309-319.

Castañeda, J. 2012. Estudio de las propiedades de trasporte en materiales porosos mediante espectroscopía infrarrojo con trasformada de fourier (FTIR). Tesis de magister en ciencias Facultad de Ciencias, Escuela de Química. Medellin, Universidad Nacional de Colombia.

Chen-Hsiu, Y.; Chih-Hung, H.; Chung-Sung, T. 2012. A Review of CO_2 Capture by Absorption and Adsorption. *Aerosol and Air Quality Research* 12: 745-769.

Da Gama, C.; Navarro-Torres, V.; Falcao-Neves, A. 2010. Techological innovations on underground coal gasification and CO_2 sequestration. *DYNA* **77**:101-108.

ECOBA. 2007. Coala Combustion Product. Production and Survey. 2013.[online] <http://www.ecoba.com/evjm,media/EUROCOALASH/01_Feuerborn.pdf.>[11 november 2013].

Gerdemann, S. J.; O'Connor, W. K.; Dahlin, D.C.; Penner, L.R.; Rush, H. 2007. Ex Situ Aqueous Mineral Carbonation. *Environmental Science & Technology* 41(7):2587-2593.

Hong, J.K.; Jo, H.Y.; Yun, S.T. 2009. Coal fly ash and synthetic coal fly ash aggregates as reactive media to remove zinc from aqueous solutions. *Journal of Hazardous Materials* 164(1):235-246.

Hoyos-Barreto, A. E.; Jiménez-Correa, M.; Ortiz-Muñoz, M.A.; Montes de Correa, C. 2008. Tecnologías para la reducción de emisiones de gases contaminantes en plantas cementeras. *Ingeniería e Investigación* 28:41-46.

Lopez-Anton, M.A.; Perry, R.; Abad-Valle, P.; Díaz-Somoano, M.; Martínez-Tarazona, M.R.; Maroto-Valer, M.M. 2011. Speciation of mercury in fly ashes by temperature programmed decomposition. *Fuel Processing Technology* 92(3):707-711.

Malik, A.; Thapliyal, A. 2009. Eco-friendly Fly Ash Utilization: Potential for Land Application. *Critical Reviews in Environmental Science and Technology* 39(4):333-366.

Maroto-Valer, M.; Lu, Z.; Zhang, Y.; Tang, Z. 2008. Sorbents for CO_2 capture from high carbon fly ashes. *Waste Management* 28(11):2320-2328.

Maroto-Valer, M.M.; Tang, Z.; Zhang, Y. 2005. CO_2 capture by activated and impregnated anthracites. *Fuel Processing Technology* 86(14-15):1487-1502.

Pevida, C.; Plaza, M.G.; Arias, B.; Fermoso, J.; Rubiera, F.; Pis, J.J. 2008. Surface modification of activated carbons for CO_2 capture. *Applied Surface Science* 254(22): 7165-7172.

Ríos, C.A.; Williams, C.D.; Roberts, C.L. 2009. A comparative study of two methods for the synthesis of fly ash-based sodium and potassium type zeolites. *Fuel* 88(8):1403-1416.

Sanz, A. 2012. Diseño de ciclos PSA para la captura de gases de combustión con adsorbentes comerciales. Tesis Doctoral. Departamento de Ingeniería Química. Universidad Complutense de Madrid. Madrid.

Sayari, A. 2010. Stabilization of Amine-Containing CO_2 Adsorbents: Dramatic Effect of Water Vapor. *Journal of the American Chemical Society* 132(18):6312-6314.

Torres-Fuchslocher, C.; Varas-Concha, F. 2015. Desing and efficiency of a small-scale woochip furnace. *Maderas. Ciencia y Tecnología* 17(2):355-364.

Vassilev, S.V. 2005. Methods for Characterization of Composition of Fly Ashes from Coal-Fired Power Stations: A Critical Overview. *Energy & Fuels* 19(3):1084-1098.

Wilcox, J. 2012. *Carbon Capture*. New York, Springer.

Xu, X.; Song, C.; Andresen, J.M.; Miller, B.G.; Scaroni, A.W. 2002. Novel Polyethylenimine-Modified Mesoporous Molecular Sieve of MCM-41 Type as High-Capacity Adsorbent for CO_2 Capture. *Energy & Fuels* 16(6):1463-1469.

Yong, Z.; Mata, V.; Rodrigues, A.R.E. 2002. Adsorption of carbon dioxide at high temperature a review. *Separation and Purification Technology* 26(2-3):195-205.

Yue, M.B.; Chun, Y.; Cao, Y.; Dong, X.; Zhu, J.H. 2006. CO_2 Capture by As-Prepared SBA-15 with an Occluded Organic Template. *Advanced Functional Materials* 16(13):1717-1722.